*Perspective*

# Calcium Sparks: Release Packets of Uncertain Origin and Fundamental Role

Natalia Shirokova,* Adom González,* Wolfgang G. Kirsch,* Eduardo Ríos,* Gonzalo Pizarro,‡ Michael D. Stern,§ and Heping Cheng§

From the *Department of Molecular Biophysics and Physiology, Rush University, Chicago, Illinois 60612; ‡Departamento de Biofísica, Facultad de Medicina, Universidad de la República, G. Flores 2125, Montevideo, Uruguay; and §Laboratory of Cardiovascular Science, Gerontology Research Center, NIA, NIH, Baltimore, Maryland 21224

$Ca^{2+}$ sparks have intrigued researchers since their discovery (Cheng et al., 1993). No one anticipated their existence; therefore, they must be telling us something we did not know. Also appealing are the esthetics of a sharp rise in local $Ca^{2+}$, extremely limited in space and time but large compared with the recording noise.

These features encouraged from early on a parsimonious interpretation of their origin and significance, including two related aspects: sparks are the result of ryanodine receptor channels (RyRs) opening individually and they are the sole form of $Ca^{2+}$ release (all release is constituted by sparks). An alternative view gained credence later, that sparks involve several (say, 20) channels opening and closing in concert. This view was fostered by observations of a release that is continuous, or constituted by events smaller than sparks, presumably reflecting the opening of individual channels. Therefore, the two views disagree as regards both the number of channels involved and existence and relevance of a nonspark form of release.

Even though the contrast between these two views attracts much of the attention, the most significant question that has to be answered, as a way of furthering our understanding of physiologic control of $Ca^{2+}$ release, contemplates the mechanisms by which sparks or other forms of release are elicited. A first answer, almost trivial for lack of alternatives in the case of cardiac muscle, is that sparks are elicited by a local increase in $[Ca^{2+}]$ calcium-induced calcium release (CICR), brought about initially by the opening of membrane L-type $Ca^{2+}$ channels.

In the case of skeletal muscle, where physiologic release requires first the activation of dihydropyridine receptors (DHPr's) operating as membrane voltage sensors, $Ca^{2+}$ appears to be the physiologic trigger of sparks as well. The evidence includes morphological similarity of sparks in both types of muscle, the observed correlation between spark frequency and myoplasmic $[Ca^{2+}]$ (Klein et al., 1996), and the effects of antagonists of CICR (tetracaine, Shirokova and Ríos, 1997; and $Mg^{2+}$, González et al., 1998).

The detection of sparks was made possible by confocal microscopy and the existence of indicators that fluoresce negligibly when free of $Ca^{2+}$ and have kinetic reaction constants that allow them to report effectively even brief events of localized release. If fluo-3 is allowed time to equilibrate, the signal $\Delta F$ that it produces relative to the initial level of fluorescence $F_0$ is proportional to the increase in $[Ca^{2+}]$ relative to the initial, resting $[Ca^{2+}]_i$. This proportionality extends, with scant saturation within a wide range of release fluxes, to the relationship between $\Delta F/F_0$ and the flux of $Ca^{2+}$ release during a simulated spark. This is shown in Fig. 1 where sparks are simulated as the result of $Ca^{2+}$ flux from a channel undergoing one 6-ms opening in a homogeneous medium with distributed $Ca^{2+}$ removal properties that copy those of myoplasmic structures (Ríos et al., 1998; and Ríos, Stern, González, Pizarro, and Shirokova, manuscript submitted for publication). Another feature of this type of simulation (Pratusevich and Balke, 1996; Smith et al., 1998; Jiang et al., 1998) is a close relationship between the release duration and the rise time of the simulated spark.

The issue of the number of channels involved in a spark has been approached by measuring morphological aspects of individual sparks (how "tall" and wide they are, and how long they last), by trying to guess how much $Ca^{2+}$ release flux would be necessary to reproduce such events, by interfering with CICR, and by quantitative modeling. These studies help evaluate the significance of sparks within the framework of excitation–contraction (E-C) coupling. This article reviews them in six brief sections.

## *How Big Is a Spark?*

Measured spark amplitude varies widely from the lower limits of detection (defined by noise, usually ~0.3 U $F_0$) to the highest values recorded, which in our experience with cut fiber segments under voltage clamp go routinely beyond 6 $F_0$ for a few sparks in every experi-


J. Gen. Physiol. © The Rockefeller University Press • 0022-1295/99/03/377/8 $2.00
Volume 113 March 1999 377–384
http://www.jgp.org

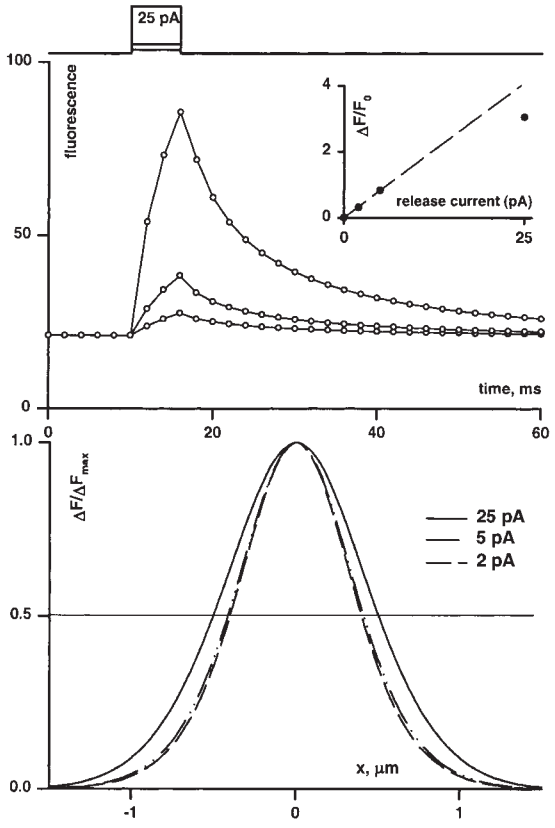


FIGURE 1. Simulations of sparks for three $Ca^{2+}$ currents represented at top, of 2, 5, and 25 pA, lasting 6 ms, originating at even density from a 0.2-μm radius sphere and entering a homogeneous medium with distributed $Ca^{2+}$ removal properties that simulate skeletal muscle. (Middle) Time dependence of fluorescence in the central pixel of simulated line scan image. (Inset) Peak increase in fluorescence, $\Delta F/F_0$, vs. current; the line is traced through the first two points. (Bottom) Normalized spatial profile at the time of maximum fluorescence. Note: (a) near linearity between peak fluorescence and release current, (b) agreement between rise time and open channel time, (c) spark amplitude within the range observed experimentally, even at the largest current, and (d) the FWHM (in spatial profile) is ~1 μm (while the experimental values are 1.5–2 μm). Details of simulation in Ríos et al. (manuscript submitted for publication). Diffusion coefficients ($\mu m^2\ ms^{-1}$): $Ca^{2+}$, 0.35; dye (free or $Ca^{2+}$-bound), 0.02; EGTA (free or $Ca^{2+}$-bound), 0.036; ATP, 0.14; parvalbumin (parv), 0.016. Association rate constants ($mM^{-1}\ ms^{-1}$): Ca:dye, 32; Ca:EGTA, 2; Ca:troponin, 5.7; Ca:ATP, 150; Ca:parv, 125; Ca:pump, 500; Mg:ATP, 1.95; Mg:parv, 0.03. Dissociation rate constants ($ms^{-1}$): Ca:dye, 0.033; Ca:EGTA, 0.002; Ca:pump, 0.5; Ca:ATP, 30; Mg:ATP, 0.195; Ca:parv, 0.0005; Mg:parv, 0.003; Ca:troponin, 0.0114. Maximum SR pump rate, 0.0098 mM/ms. Total concentrations (mM):dye, 0.15; pump sites, 0.24; parv, 1; troponin, 0.24; EGTA, 1; ATP, 5; [$Mg^{2+}$], 0.15 (taken to be constant). Spark blurred with $FWHM_x = FWHM_y = 0.33\ \mu m$, $FWHM_z = 1.0\ \mu m$.

ment. Current work with cardiac myocytes and smooth muscle also finds events of amplitude >5, much larger than in earlier reports (Wier et al., 1999). In our experience amplitudes are substantially lower in fibers permeabilized by saponin or by notches and immersed in internal solution (a preparation described by Lacampagne et al., 1998).

The reason for the differences in amplitude may be quite simple: as stated, $\Delta F/F_0$ is close to the ratio between increase in local [$Ca^{2+}$] and resting [$Ca^{2+}$]$_i$. The cell may be able to maintain a substantially lower internal $Ca^{2+}$ in the voltage clamp experiments, which expose it to internal solution at the cut ends only. By contrast, in permeabilized fiber segments, free [$Ca^{2+}$] should equilibrate rapidly within the cell at the solution value, and the dye rises rapidly, reaching values higher than the concentration in the internal solution. Therefore, the relative increase $\Delta F/F_0$ (or $\Delta$[$Ca^{2+}$]/resting [$Ca^{2+}$]) should be less in the permeabilized fibers due to the buffering effect of the higher [dye] (which reduces $\Delta$[$Ca^{2+}$]) and the higher resting [$Ca^{2+}$]. Indeed, sparks with very large values of $\Delta F/F_0$ are only found early in voltage clamp experiments, when the resting fluorescence is very low (indicating low dye concentration, low [$Ca^{2+}$], or both).

In our first study of discrete events (Tsugorka et al., 1995), we evaluated event amplitude by constructing all-points histograms of the difference records between fluorescence at triadic centers and in the neighboring sarcomeres. The resulting histograms had modes at between 0.1 and 0.3 $F_0$, which were interpreted as spark amplitudes. We now believe that the all-points histogram is not an adequate tool to recognize sparks because it does not take into account their multidimensional aspects. When their frequency is low, sparks will contribute negligibly to the all-points histogram, which should be dominated by very small fluctuations that may correspond to out-of-focus sparks or to continuous, eventless release. In fact, when automatic procedures are used with an amplitude selection criterion (see next section), the resulting histograms also peak at or near the lowest allowed amplitude. Therefore, modes in the amplitude distributions will always be at very small values regardless of the true amplitude of the events. We now prefer methods of recognition by multidimensional criteria (amplitude, width, duration). Such recognition was initially done by an observer (Cheng et al., 1993; Klein et al., 1996; Shirokova and Ríos, 1997), but is now entirely automatic (Cheng et al., 1999), and yields amplitude estimates at least an order of magnitude greater.

The width of large sparks (measured as full width at half magnitude, FWHM) varies between 1.5 and 2.2 μm in skeletal muscle. In cardiac muscle, where some sparks appear to result from multiple release sources (Parker et al., 1996; Blatter et al., 1997) and can be very wide, there is a well defined subset of sparks that appear to originate from single release sites. The half width of those is similar to that in skeletal muscle, ~2 μm. Surprisingly, and as shown in Fig. 1, in simulations of

sparks resulting from a discrete $Ca^{2+}$ source the half width is only ~1 μm, regardless of assumptions on the properties of buffers and the dye. The width of the simulated spark could be increased to reach values near 2 μm by increasing the radius of the source (to 1 μm). The discrepancy and its resolution may be taken as evidence that the source of release is extensive (rather than a single channel), or it may mean that the models of $Ca^{2+}$ release and removal are inadequate in ways we do not understand.

### *$Ca^{2+}$ Release Flux Underlying a Spark*

This has been calculated in cardiac (Blatter et al., 1997; Lukyanenko et al., 1998) and skeletal muscle (Ríos et al., 1998; manuscript submitted for publication) by generalizing global or whole-cell procedures of Baylor et al. (1983) and Melzer et al. (1984, 1987) to the spatially resolved images obtained by confocal microscopy. The earlier procedures first derive from the optical signals the transient increase in free $[Ca^{2+}]$, and then calculate the increase in total calcium necessary to account for such transient by adding contributions from different $Ca^{2+}$ binding and removal processes. They are therefore subject to errors in the calculation of free $[Ca^{2+}]$ and in the ulterior estimate of binding and removal. The generalization to sparks has additional uncertainties regarding diffusional mobility of the different $Ca^{2+}$ ligands and placement of fixed sites. If calculations are carried out assuming a homogeneous and unrestricted distribution of sites, with consensus values for concentrations, diffusion coefficients, and reaction rate constants, the values obtained are typically near 10 pA, and often >20 pA for the largest sparks in every image.

A lower bound of released $Ca^{2+}$ can be obtained without calculating local $[Ca^{2+}]$, based on the rate of $Ca^{2+}$ binding to the dye that is needed to account for the observed fluorescence. Take as numeric example a permeabilized fiber equilibrated with a 100 nM free $[Ca^{2+}]$, 200 μM fluo-3 solution, at a time when the internal dye concentration has risen to 300 μM. In this condition, the resting fluorescence corresponds to ~30 μM of the dye:Ca complex (assuming that the dye reacts inside the fiber with a $K_d$ of 1 μM, the low end of the range estimated by Harkins et al., 1993). A large spark under these conditions may have an amplitude of 2.5 $F_0$, requiring an additional 75 μM of dye-bound $Ca^{2+}$. The quantity of dye-bound $Ca^{2+}$ can be found by volume integration of concentration, roughly the product of peak value by the volume of the sphere that intersects the spark at half magnitude, say 1.8 μm. Thus, 75 μM × 3.05 $\mu m^3$ or 0.23 amol $Ca^{2+}$, equivalent to 43.4 fC, must be released within the rise time of the spark, 5 ms. Therefore, an average current close to 10 pA must flow for 5 ms just to account for the $Ca^{2+}$ bound to the dye in this example. Such values are typical of large sparks in experiments with permeabilized fibers.

The free $[Ca^{2+}]$ in cardiac SR was estimated using $^{19}F$ NMR at 1.5 mM (Chen et al., 1996). Mejía-Alvarez et al. (1999) used the result to estimate the physiologic current-carrying capability of cardiac release channels, measuring their $Ca^{2+}$ current in bilayers, with a luminal side $[Ca^{2+}]$ of 2 mM and in the presence of concentrations of $Cs^+$ comparable to physiologic $[K^+]$. Under those conditions, the average unitary current was 0.35 pA. Extrapolated to the case of skeletal muscle, this estimate indicates that tens of channels should be open to account for large sparks.

Though lower than in earlier work (Tinker et al., 1992), these estimates of current per channel are consistent with whole-cell measures of release flux. The maximum flux density (expressed as rate of rise of total calcium concentration in the accessible myoplasmic volume) under voltage clamp in the frog is between 180 and 200 mM/s (Pape et al., 1995; Shirokova and Ríos, 1996). The volume density of release channels can be gathered from morphometry. The ratio of transverse tubule length to fiber volume is 0.82 $\mu m^{-2}$ in frog muscle (Eisenberg and Peachey, 1975). If 70% of this length is junctional and contains a double row of release channels at 30 nm spacing on each side (Block et al., 1988), the number of channels per liter is 0.82 $\mu m^{-2}$ (tubule length/fiber volume) × 0.7 (triad length/tubule length), × 2 (junctions/triad), × 2 (rows/junction), × 33 (channels/row/μm), or 1.08 × $10^{17}$ channels per liter of fiber. At 100% activation, such channels passing 0.35 pA would generate a flux density of 180 mmol/liter of fiber per s, or 260 mM/s in terms of accessible aqueous myoplasmic volume, surpassing the highest whole-cell estimates.

### *The Distribution of Spark Amplitudes*

The appeal of sparkology, as we stated, is to some extent esthetic—images with sparse sparks, in a dark experimental room, look very much like a starry sky. Much as stars in the sky, small sparks greatly outnumber the large ones, and the reasons for this are not very different for sparks and stars. Indeed, sparks are recorded in line scans, but may originate anywhere within the junctions of a Z disk. The smoothly decaying point spread function of the imaging system implies that the sparks originating farther from the scanned line will appear smaller in the record. And the regions of Z disk that lie "far" are greater than those that are "near," hence the probability density function of spark amplitudes is expected to be decaying, even if sparks as objects are all of the same size.

The above reasoning led two groups to derive, using different formal approaches, the distribution of ampli-

tudes expected in a line scan image for identical sparks that originate with homogeneous probability in triadic locations (Izu et al., 1998; Cheng et al., 1999). This function is a simple inverse proportionality (pdf $\propto a^{-1}$, where $a$ is recorded amplitude).

In agreement with theory, the amplitude histograms of events identified by a program that locates them without human intervention (Cheng et al., 1999) are monotonically decreasing. The dependence of frequency on amplitude, however, is not the inverse function predicted for identical sparks, being consistent instead with a widely spread distribution of real spark amplitudes. The distribution of real spark amplitudes (derived by a method of González et al., 1999, which corrects for the effect of line scanning) exhibits in the presence of caffeine a mode or preferred amplitude at between 2 and 3 $F_0$.

With this improved understanding of the meaning of recorded spark amplitude, it is natural to use large sparks, rather than those of average size, to estimate release flux, because the large ones are more likely originated near the scanned line, where recorded amplitudes are greatest. Because there is a spread of actual amplitudes, the largest sparks, whose underlying release current was estimated at >20 pA, may be outliers of unusually large amplitude as objects. For the sparks of the most common size, one third of the above estimate should apply, or ~7 pA.

### *Beyond Sparks*

The above considerations, plus the structural evidence that release channels are clustered in closely packed arrays, in skeletal (Block et al., 1988) as well as cardiac muscle (Sun et al., 1995), present a problem if single channels gate individually to produce sparks. How can a release channel pass the spark current (somewhere between 1 and 30 pA) without activating other channels that face the same junctional gap, where [$Ca^{2+}$] would rapidly rise beyond 100 μM (Langer and Peskoff, 1996; Stern et al., 1997)? The argument was bolstered by the demonstration in cardiac muscle of coupled fluorescence events in scans perpendicular to the fiber axis (Parker et al., 1996) and of multiple sources of release under large sparks of cat atria (Blatter et al., 1997). Both observations show that the activation of cardiac release channels, presumably by $Ca^{2+}$, occasionally reaches across distances of 1 μm or more, stressing that single $Ca^{2+}$-activatable channels within a junction can hardly operate independently.

A many-channel origin for sparks was supported by the observation in ventricular myocytes of a diffuse increase in fluorescence, devoid of sparks, when trigger $Ca^{2+}$ was delivered by photolysis of DM-nitrophen (Lipp and Niggli, 1996). The authors hypothesized that thus triggered SR $Ca^{2+}$ release was composed by contributions (termed quarks) that could not be individually detected. Although the terminology is intriguing, skeletal muscle soon forced consideration of another alternative, continuous release.

In skeletal muscle, an increase in fluorescence not composed of sparks can be readily demonstrated under a number of conditions. When slightly depolarized, some frog fibers show at triads release not constituted by discrete events, while typical sparks appear at higher voltages (Shirokova and Ríos, 1997). In tetracaine at 200 μM, which blocks release channels in bilayers (Xu et al., 1993), depolarization triggers continuous release but no sparks (Shirokova and Ríos, 1997).

In mammalian muscle of adult rats, voltage-clamp depolarization caused continuous $Ca^{2+}$ release and contraction, but no sparks (Shirokova et al., 1998). The triadic origin of the release was demonstrated by the existence of a triadic gradient of fluorescence (which is nearly proportional to release flux; Tsugorka et al., 1995). Because the gradients of fluorescence associated with continuous release in both frogs and rats could be much lower than in sparks, it appears that continuous release may involve smaller currents, again indicating the participation of channel groups in the production of sparks.

Shirokova and Ríos (1997) interpreted the continuous release observed in frogs at very low voltages or in the presence of tetracaine as flux through channels directly operated by voltage sensors. They proposed that sparks are the consequence of opening of multiple channels, caused by a local increase in [$Ca^{2+}$]. This increase would be started in frog skeletal muscle by release channels operated by voltage-sensing DHPrs, and reinforced by the opening of additional channels. The directly voltage-operated release component could appear alone, without triggering CICR and sparks, if the concentration of trigger $Ca^{2+}$ was insufficient (e.g., at low voltage depolarization) or the sensitivity to $Ca^{2+}$ was inhibited (in the tetracaine experiment). This hypothesis also explains why it is so difficult to demonstrate nonspark release in cardiac muscle, where presumably there is no direct activation of release by voltage.

Rat muscle provides an example of eventless release (Shirokova et al., 1998) that is most interesting for various reasons. The failure to observe sparks there could simply evidence difficulties in working with smaller, weaker cells, cut (Hollingworth et al., 1996), and at far from physiologic temperature. We believe instead that the absence of sparks in adult rats reflects a fundamental difference in the E-C coupling mechanism, consistent with differences found in whole cell experiments (Shirokova et al., 1996). These differences include a lesser peak of $Ca^{2+}$ release flux, a lower ratio between the peak and steady levels of release under voltage

clamp, the absence in the rat of the characteristic voltage dependence of this ratio observed in the frog, and the presence in the rat (Suda and Penner, 1994), but not in the frog (Shirokova and Ríos, 1996), of the RISC phenomenon, a stop by repolarization of the release induced by caffeine.

RISC is interpreted as indicating a preponderance of control by membrane voltage (via the DHPr). Its presence in the rat, and failure to appear in the frog, are consistent with our failure to demonstrate sparks (which presumably are mediated by CICR) in rats, and the ease with which continuous, voltage-operated release can be demonstrated in the mammal. In all, it appears that CICR is fundamental in the frog, where it determines sparks and the pronounced, steeply voltage-dependent peak of the release waveform, while it is much less important, perhaps absent, in the rat. Because sparks were present in myotubes from embryonic or neonatal mice, which unlike adult cells express RyR isoform 3, Shirokova et al. (1998) proposed that the production of sparks could require RyR3 (or the corresponding β isoform in frog muscle). This possibility is now bolstered by the observation of sparks in dyspedic mouse cells expressing RyR3 but not RyR1 (see Schneider, 1999, in this issue).

Finally, the molecular makeup of frog triads is usually assumed to be the same as that in mammals, but this may not be the case. The ratio of ryanodine-binding sites to DHPrs expected from the structural model of Block et al. (1988), in which four voltage sensors face every other release channel, is 0.5. This value is found approximately in membrane fractions of rabbit or human muscle (Bers and Stiffel, 1993; Margreth et al., 1993; Anderson et al., 1994). In frogs, the value is ~1.5 (Margreth et al., 1993; Anderson et al., 1994), which would suggest an excess of release channels, either outside the double row or violating the pattern in some other way. The possibility of major structural differences must be kept in mind, as the morphological alignment of mammalian and fish junctions has never been confirmed in the frog (Franzini-Armstrong and Jorgensen, 1994).

### *Models of Spark Generation*

The "couplon" model (Stern et al., 1997) is the latest of a class that assumes interactions within arrays of channels. The couplon, consisting of the contiguous array of RyRs associated with one side of a junctional segment of transverse tubule, includes two rows of RyRs that alternate between those associated with a DHPr tetrad, presumed to be controlled only by voltage (V channels), and those lacking contact with DHPrs, which are assumed to be activated and inactivated by $Ca^{2+}$ alone (C channels). With suitable parameters, this model reproduces many of the global features of frog skeletal muscle E-C coupling (including its "quantal" aspects; Pizarro et al., 1997), which would be difficult to explain if release resulted from channels gating independently.

The couplon model normally generates spark-like release packets. Openings of V channels trigger, by CICR, openings of adjacent C channels, which in turn may recruit other C channels. The whole couplon, or a part of it, may thus activate to generate a phenomenon similar to a spark. Given the assumed C channel unitary current, 0.3 pA, and the size of a couplon (10–30 C channels), the simulated spark sizes are consistent with the observations. Most interestingly, the couplon sparks have a preferred amplitude (Stern et al., 1997), in agreement with amplitude distributions obtained by González et al. (1999) in the presence of caffeine.

Could single channel openings produce sparks with a preferred amplitude? As shown in Fig. 1, the amplitude of a spark due to a single channel opening should be nearly proportional to the opening duration. For a single Markovian channel, gating reversibly, the distribution of open times is a sum of positively weighted decaying exponentials (Colquhoun and Hawkes, 1995), so a mode in the distribution of amplitudes would not be expected. However, RyRs of striated muscle can be activated by its own permeating $Ca^{2+}$ under suitable conditions in lipid bilayers (Tripathy and Meissner, 1995; Xu and Meissner, 1998). This would couple the free energy of $Ca^{2+}$ permeating down its electrochemical gradient to the gating process, permitting irreversible gating kinetics and open time distributions with a mode (Colquhoun and Hawkes, 1995).

The couplon simulations reproduce the sharp peak observed in whole-cell determinations of $Ca^{2+}$ release in the frog as essentially a sum of sparks, while the steady level that follows the peak is accounted for as a combination of sparks and continuous, directly voltage-operated release. This picture of the peak of release as composed of sparks and mediated by CICR justifies that tetracaine eliminates sparks together with the peak (Shirokova and Ríos, 1997), and that the peak can be reconstructed by superposition of sparks whose timing is determined in fibers with partially inactivated voltage sensors (Klein et al., 1997).

The couplon, and related multichannel models, explain the increase of the peak relative to the steady level as voltage is increased, as a result of cooperation of multiple voltage-operated sources within the same couplon to produce a level of $Ca^{2+}$ that will elicit sparks. Such models predict that partial inactivation of voltage sensors or interference with CICR may be compensated by recruiting more voltage sensors, hence explaining that DHPr antagonists (Shirokova and Ríos, 1997), high intracellular $Mg^{2+}$ (Kirsch et al., 1999), or

BAPTA (Brum and Pizarro, 1998), inhibit sparks or the peak phase of release at low, but not at high voltages.

The most parsimonious model (release entirely composed of sparks reflecting opening of one or two channels operated by one voltage sensor) is ruled out by its prediction that disabling some voltage sensors would just scale down release and spark numbers. Instead, the waveform reconstructed in partially inactivated fibers (Klein et al., 1997) showed a much smaller steady component of release flux at high voltage than in fully primed fibers (Pape et al., 1995; Shirokova et al., 1996), which again suggests the existence of a voltage-operated release not in discrete events, and required higher voltages to produce a peak of release (compared with fully primed fibers; Klein et al., 1996), which again indicates cooperation among multiple voltage sensors to activate the same release unit.

### *Terminating the Spark*

As we stated at the outset, sparks were not expected. Their spatial discreteness could have been predicted on structural grounds (in fact, spatially segregated release at triads had been demonstrated earlier by Escobar et al., 1994), but their temporal brevity was startling. Rise times of sparks, which roughly measure release duration, are quite independent of triggering voltage, partial inactivation (Klein et al., 1997), or $Ca^{2+}$ channel blockers (López-López et al., 1995; Santana et al., 1996), which suggests a termination mechanism intrinsic to the release unit, rather than the trigger.

The models of spark generation described above underscore the difficulties in devising a mechanism with robust termination. Local depletion of SR $Ca^{2+}$ has been ruled out in cardiac myocytes because $Ca^{2+}$ sparks may last up to a few seconds (Cheng et al., 1993; Parker and Wier, 1997; Xiao et al., 1997; Lukyanenko et al., 1998). In skeletal and cardiac muscle, images of sparks arising repetitively from the same unit also indicate that depletion does not determine spark termination. Sham et al. (1998) examined the issue in cardiac myocytes, where sparks are triggered by $Ca^{2+}$ influx through membrane channels. Observing that reopenings of membrane $Ca^{2+}$ channels, even with duration greatly prolonged by FPL64176, failed to trigger $Ca^{2+}$ release, they concluded that the termination mechanism includes desensitization to the trigger. Furthermore, they showed that this loss of sensitivity is not an adaptation (in the sense proposed by Györke and Fill, 1993, whereby channels that lose sensitivity can be reactivated by higher [$Ca^{2+}$]) because $Ca^{2+}$ release activated by the tail membrane current at the end of a pulse involved only channels that were not activated at the beginning of the pulse. Taken together, these results indicate that $Ca^{2+}$ sparks are terminated primarily by inactivation of RyRs. It remains to be established whether the inactivation is a $Ca^{2+}$-dependent process (Fabiato, 1985; Schneider and Simon, 1988; Jong et al., 1995), or is "fatal" (Pizarro et al., 1997), an obligatory coda to channel opening.

In any case, the implementation of such mechanisms is more difficult if sparks are multichannel events, simply because it is more difficult to turn-off many channels synchronously. Inter-channel allosteric interactions (Marx et al., 1998) might help, channel closing could be synchronized by negative interactions between RyRs in the quasi-crystal of the junction (Stern et al., 1999).

In summary, sparks appear to constitute the totality of physiologic $Ca^{2+}$ release in cardiac muscle, and a major portion of it in frog skeletal muscle. The early peak of release during a voltage pulse is largely constituted by a superposition of sparks, a conclusion that can probably be extrapolated to release in response to an action potential. Release not constituted by separable events is found under various conditions in skeletal muscle; it might be the trigger of sparks in frogs, and the sole form of release in mammals. The origin of sparks is unsettled. The release flux estimated for the largest sparks seems too high to be carried by just one channel. The shift of voltage dependence of spark activation upon partial inactivation of voltage sensors and other complex properties of the whole-cell release waveform are better understood if channels engage in group interactions. Finally, if sparks were one-channel events, it would be difficult to explain why most release channels would consistently fail to activate when facing the high triadic gap [$Ca^{2+}$] associated with a typical spark. On the other hand, the rapid and effective termination of individual sparks can be more easily justified if sparks result from the opening of individual release channels. The distribution of spark amplitudes corrected for the distorting effects of line scanning may exhibit a modal amplitude, which is more easily explained with multichannel models of sparks, but may also be a feature of single channels that gate irreversibly. In general, it is very difficult to account for the properties of sparks, or whole-cell $Ca^{2+}$ release, by simply extrapolating the properties of individual channels in bilayers, which suggests that interactions with other triadic proteins, including release channels, and other forms of local modulation, may crucially influence physiologic gating.

Many questions therefore remain unanswered. Going back to the stars metaphor, the trek is far from over.

We are grateful to W.G. Wier for making his unpublished work available to us.

This work was supported by grants from the National Institutes of Health (NIH) to E. Ríos, a grant from NIH to Philip Palade and M.D. Stern, a grant from NIH to N. Shirokova, and intramural research programs of NIH to M.D. Stern and H. Cheng. A. González was the recipient of a Senior Fellowship from the American Heart Association of Metropolitan Chicago.

*Original version received 7 December 1998 and accepted version received 8 January 1999.*

## REFERENCES

Anderson, K., A.H. Cohn, and G. Meissner. 1994. High-affinity [$^3$H]PN200-110 and [$^3$H]ryanodine binding to rabbit and frog skeletal muscle. *Am. J. Physiol.* 266:C462–C466.

Baylor, S.M., W.K. Chandler, and M.W. Marshall. 1983. Sarcoplasmic reticulum calcium release in frog skeletal muscle fibres estimated from Arsenazo III calcium transients. *J. Physiol. (Lond.).* 344:625–666.

Bers, D.M., and V.M. Stiffel. 1993. Ratio of ryanodine to dihydropyridine receptors in cardiac and skeletal muscle and implications for E-C coupling. *Am. J. Physiol.* 264:C1587–C1593.

Blatter, L.A., J. Hüser, and E. Ríos. 1997. Sarcoplasmic reticulum $Ca^{2+}$ release flux underlying $Ca^{2+}$ sparks in cardiac muscle. *Proc. Natl. Acad. Sci. USA.* 94:4176–4181.

Block, B.A., T. Imagawa, K.P. Campbell, and C. Franzini-Armstrong. 1988. Structural evidence for direct interaction between the molecular components of the transverse tubule/sarcoplasmic reticulum junction in skeletal muscle. *J. Cell Biol.* 107:2587–2600.

Brum, G., and G. Pizarro. 1988. Pharmacology of $Ca^{2+}$ release in the presence of high intracellular [BAPTA] in frog skeletal muscle. *Biophys. J.* 74:A166.

Chen, W., C. Steenbergen, L.A. Levy, J. Vance, R.E. London, and E. Murphy. 1996. Measurements of free $Ca^{2+}$ on sarcoplasmic reticulum in perfused rabbit heart loaded with 1,2-bis (2-amino-5,6-difluorophenoxy)ethane-*N,N,N′,N′*-tetraacetic acid by 19F NMR. *J. Biol. Chem.* 271:7398–7403.

Cheng, H., W.J. Lederer, and M.B. Cannell. 1993. Calcium sparks: elementary events underlying excitation–contraction coupling in heart muscle. *Science.* 262:740–744.

Cheng, H., L.S. Song, N. Shirokova, A. González, E.G. Lakatta, E. Ríos, and M.D. Stern. 1999. Amplitude distribution of calcium sparks in confocal images. Theory and studies with an automatic detection method. *Biophys. J.* 76:606–617.

Colquhoun, D., and A.G. Hawkes. 1995. The principles of the stochastic interpretation of ion-channel mechanisms. *In* Single-Channel Recording. B. Sakmann and E. Neher, editors. Plenum Publishing Corp., New York. 397–484.

Eisenberg, B.R., and L.D. Peachey. 1975. The network parameters of the T-system in frog muscle measured with the high voltage electron microscope. *In* 335th Annual Proceedings of the Electron Microscopy Society of America. G.W. Bailey, editor. p. 550.

Escobar, A.L., J.R. Monck, J.M. Fernandez, and J.M. Vergara. 1994. Localization of the site of $Ca^{2+}$ release at the level of a single sarcomere in skeletal muscle fibres. *Nature.* 367:739–741.

Fabiato, A. 1985. Time and calcium dependence of activation and inactivation of calcium-induced release of calcium from the sarcoplasmic reticulum of a skinned canine cardiac Purkinje cell. *J. Gen. Physiol.* 85:247–289.

Franzini-Armstrong, C., and A.O. Jorgensen. 1994. Structure and development of E-C coupling units in skeletal muscle. *Annu. Rev. Physiol.* 56:509–534.

González, A., N. Shirokova, W.G. Kirsch, and E. Ríos. 1998. High intracellular [$Mg^{2+}$] affects whole cell $Ca^{2+}$ release and its elementary events in skeletal muscle. *Biophys. J.* 74:A234.

González, A., N. Shirokova, W.G. Kirsch, G. Pizarro, M.D. Stern, H. Cheng, and E. Ríos. 1999. Size distribution of $Ca^{2+}$ sparks in caffeine-stimulated skeletal muscle. *Biophys. J.* 76:A385.

Gÿorke, S., and M. Fill. 1993. Ryanodine receptor adaptation: control mechanism of $Ca^{2+}$ induced $Ca^{2+}$ release in heart. *Science.* 260:807–809.

Harkins, A.B., N. Kurebayashi, and S.M. Baylor. 1993. Resting myoplasmic free calcium in frog skeletal muscle fibers estimated with fluo-3. *Biophys. J.* 65:865–881.

Hollingworth, S., M. Zhao, and S.M. Baylor. 1996. The amplitude and time course of the myoplasmic free [$Ca^{2+}$] transients in fast-twitch fibers of mouse muscle. *J. Gen. Physiol.* 108:455–469.

Izu, L.T., W.G. Wier, and C.W. Balke. 1998. Theoretical analysis of the $Ca^{2+}$ spark amplitude distribution. *Biophys. J.* 75:1144–1162.

Jiang, Y.H., M.G. Klein, and M.F. Schneider. 1998. Numerical simulation of $Ca^{2+}$ "sparks" in skeletal muscle. *Biophys. J.* 74:A269.

Jong, D.S., P.C. Pape, S.M. Baylor, and W.K. Chandler. 1995. Calcium inactivation of calcium release in frog cut muscle fibers that contain millimolar EGTA or Fura2. *J. Gen. Physiol.* 106:337–388.

Kirsch, W.G., A. González, G. Pizarro, N. Shirokova, and E. Ríos. 1999. Rattifying the frog: effects of high intracellular [$Mg^{2+}$] on global $Ca^{2+}$ release in skeletal muscle. *Biophys. J.* 76:A385.

Klein, M.G., H. Cheng, L.F. Santana, Y.H. Jiang, W.J. Lederer, and M.F. Schneider. 1996. Two mechanisms of quantized calcium release in skeletal muscle. *Nature.* 379:455–458.

Klein, M.G., A. Lacampagne, and M.F. Schneider. 1997. Voltage dependence of the pattern and frequency of discrete $Ca^{2+}$ release events after brief repriming in frog skeletal muscle. *Proc. Natl. Acad. Sci. USA.* 94:11061–11066.

Lacampagne, A., M.G. Klein, and M.F. Schneider. 1998. Modulation of the frequency of spontaneous sarcoplasmic reticulum $Ca^{2+}$ release events ($Ca^{2+}$ sparks) by myoplasmic [$Mg^{2+}$] in frog skeletal muscle. *J. Gen. Physiol.* 111:207–224.

Langer, G.A., and A. Peskoff. 1996. Calcium concentration and movement in the diadic cleft space of the cardiac ventricular cell. *Biophys. J.* 70:1169–1182.

Lipp, P., and E. Niggli. 1996. Submicroscopic calcium signals as fundamental events of excitation–contraction coupling in guinea-pig cardiac myocytes. *J. Physiol. (Camb.).* 492:31–38.

López-López, J.R., P.S. Shacklock, C.W. Balke, and W.G. Wier. 1995. Local calcium transient triggered by single L-type $Ca^{2+}$ channel currents in cardiac cells. *Science.* 268:1042–1045.

Lukyanenko, V., T.F. Wiesner, and S. Gÿoke. 1998. Termination of $Ca^{2+}$ release during $Ca^{2+}$ sparks in rat ventricular myocytes. *J. Physiol. (Camb.).* 507:667–677.

Margreth, A., E. Damiani, and G. Tobaldin. 1993. Ratio of dihydropyridine to ryanodine receptors in mammalian and frog twitch muscles in relation to the mechanical hypothesis of excitation–contraction coupling. *Biochem. Biophys. Res. Commun.* 197:1303–1311.

Marx, S.O., K. Ondrias, and A.R. Marks. 1998. Coupled gating between individual skeletal muscle $Ca^{2+}$ release channels. *Science.* 281:818–821.

Mejía-Alvarez, R., C. Kettlun, E. Ríos, M.D. Stern, and M. Fill. 1999. Unitary $Ca^{2+}$ current trough cardiac ryanodine receptor channels under quasi-physiological ionic conditions. *J. Gen. Physiol.* 113:177–186.

Melzer, W., E. Ríos, and M.F. Schneider. 1984. Time course of calcium release and removal in skeletal muscle fibers. *Biophys. J.* 45: 637–641.

Melzer, W., E. Ríos, and M.F. Schneider. 1987. A general procedure for determining the rate of calcium release from the sarcoplasmic reticulum in skeletal muscle fibers. *Biophys. J.* 51:849–863.

Pape, P.C., D.S. Jong, and W.K. Chandler. 1995. Calcium release and its voltage dependence in frog cut muscle fibers equilibrated with 20 mM EGTA. *J. Gen. Physiol.* 106:259–336.

Parker, I., W.J. Zang, and W.G. Wier. 1996. $Ca^{2+}$ sparks involving multiple $Ca^{2+}$ release sites along Z-lines in rat heart cells. *J. Physiol. (Camb.).* 497:31–38.

Parker, I., and W.G. Wier. 1997. Variability in frequency and characteristics of $Ca^{2+}$ sparks at different release sites in rat ventricular myocytes. *J. Physiol. (Camb.).* 505:337–344.

Pizarro, G., N. Shirokova, A. Tsugorka, and E. Ríos. 1997. 'Quantal' calcium release operated by membrane voltage in frog skeletal muscle. *J. Physiol. (Camb.).* 501:289–303.

Pratusevich, V.R., and C.W. Balke. 1996. Factors shaping the confocal image of the calcium spark in cardiac muscle cells. *Biophys. J.* 71:2942–2957.

Ríos, E., M.D. Stern, A. González, and N. Shirokova. 1998. Release flux underlying $Ca^{2+}$ sparks in frog skeletal muscle. *Biophys. J.* 74: A234.

Santana, L.F., H. Cheng, A.M. Gómez, M.B. Cannell, and W.J. Lederer. 1996. Relation between the sarcolemmal $Ca^{2+}$ current and $Ca^{2+}$ sparks and local control theories for cardiac excitation–contraction coupling. *Circ. Res.* 78:165–171.

Schneider, M.F. 1999. Perspective: $Ca^{2+}$ sparks in frog skeletal muscle: generation by one, some, or many SR $Ca^{2+}$ release channels? *J. Gen. Physiol.* 113:365–371.

Schneider, M.F., and B.J. Simon. 1988. Inactivation of calcium release from the sarcoplasmic reticulum in frog skeletal muscle. *J. Physiol. (Camb.).* 405:727–745.

Sham, J., L.S. Song, L.H. Deng, Y. ChenIzu, E.G. Lakatta, M.D. Stern, and H. Cheng. 1998. Termination of $Ca^{2+}$ release by local inactivation of ryanodine receptors in cardiac myocytes. *Proc. Natl. Acad. Sci. USA.* 95:15096–15101.

Shirokova, N., and E. Ríos. 1996. Activation of $Ca^{2+}$ release by caffeine and voltage in frog skeletal muscle. *J. Physiol. (Camb.).* 493: 317–339.

Shirokova, N., J. García, G. Pizarro, and E. Ríos. 1996. $Ca^{2+}$ release from the sarcoplasmic reticulum compared in amphibian and mammalian skeletal muscle. *J. Gen. Physiol.* 107:1–18.

Shirokova, N., and E. Ríos. 1997. Small event $Ca^{2+}$ release: a probable precursor of $Ca^{2+}$ sparks in frog skeletal muscle. *J. Physiol. (Camb.).* 502:3–11.

Shirokova, N., J. García, and E. Ríos. 1998. Local calcium release in mammalian skeletal muscle. *J. Physiol. (Camb.).* 512:377–384.

Smith, G.D., J.E. Keizer, J.D. Stern, W.J. Lederer, and H. Cheng. 1998. A simple numerical model of calcium spark formation and detection in cardiac myocytes. *Biophys. J.* 75:15–32.

Song, L.S., M.D. Stern, E.G. Lakatta, and H. Cheng. 1997. Partial depletion of sarcoplasmic reticulum calcium does not prevent calcium sparks in rat ventricular myocytes. *J. Physiol. (Camb.).* 505:665–675.

Stern, M.D., G. Pizarro, and E. Ríos. 1997. Local control model of excitation-contraction coupling in skeletal muscle. *J. Gen. Physiol.* 110:415–440.

Stern, M.D., L.S. Song, H. Cheng, J. Sham, H.T. Yang, K.R. Boheler, and E. Ríos. 1999. Local control models of cardiac excitation–contraction coupling: a possible role for allosteric interactions between ryanodine receptors. *J. Gen. Physiol.* 113:469–489.

Suda, N., and R. Penner. 1994. Membrane repolarization stops caffeine-induced $Ca^{2+}$ release in skeletal muscle cells. *Proc. Natl. Acad. Sci. USA.* 91:5725–5729.

Sun, X.H., F. Protasi, M. Takahashi, H. Takeshima, D.G. Ferguson, and C. Franzini-Armstrong. 1995. Molecular architecture of membranes involved in excitation–contraction coupling of cardiac muscle. *J. Cell Biol.* 129:659–671.

Tinker, A., A.R.G. Lindsay, and A.J. Williams. 1992. A model for ionic conduction in the ryanodine receptor channel of sheep cardiac muscle sarcoplasmic reticulum. *J. Gen. Physiol.* 100:495–517.

Tripathy, A., and G. Meissner. 1996. Sarcoplasmic reticulum luminal $Ca^{2+}$ has access to cytosolic activation and inactivation sites of skeletal muscle $Ca^{2+}$ release channel. *Biophys. J.* 70:2600–2615.

Tsugorka, A., E. Ríos, and L.A. Blatter. 1995. Imaging elementary events of calcium release in skeletal muscle cells. *Science.* 269: 1723–1726.

Wier, W.G., J.R.H. Mauban, V. Miriel, and M.B. Blaustein. 1999. $Ca^{2+}$ sparks in smooth muscle cells of pressurized arteries. *Biophys. J.* 76:A291.

Xiao, R.P., H.H. Valdivia, K. Bogdanov, C. Valdivia, E.G. Lakatta, and H. Cheng. 1997. The immunophilin FK506 binding protein modulates $Ca^{2+}$ release channel closure in rat heart. *J. Physiol. (Camb.).* 500:343–354.

Xu, L., R. Jones, and G. Meissner. 1993. Effects of local anesthetics on single channel behavior of skeletal muscle calcium release channel. *J. Gen. Physiol.* 101:207–233.

Xu, L., and G. Meissner. 1998. Regulation of cardiac muscle $Ca^{2+}$ release channel by sarcoplasmic reticulum luminal $Ca^{2+}$. *Biophys. J.* 75:2302–2312.